The influence of the Plata River discharge on the western South Atlantic shelf

Alberto R. Piola,[1] Ricardo P. Matano,[2] Elbio D. Palma,[3] Osmar O. Möller Jr.,[4] and Edmo J. D. Campos[5]

Received 29 September 2004; revised 25 November 2004; accepted 9 December 2004; published 6 January 2005.

[1] The influence of the Plata, the second largest river in South America, extends along a coastal strip of 1300 km. Historical hydrographic and wind data and numerical simulations are combined to determine the seasonal and interannual variability of the Plata plume and its relationship to the magnitude of the river discharge and the intensity and direction of the wind stress. Our results indicate that the seasonal variability of the river plume is controlled by the alongshore component of the wind stress. During El Niño the effects of the wind and precipitation anomalies tend to compensate each other, preventing anomalous northeastward plume extensions associated to large outflow events. Numerical experiments confirm this finding and indicate that during El Niño the discharge from the Plata River spreads offshore. **Citation:** Piola, A. R., R. P. Matano, E. D. Palma, O. O. Möller Jr., and E. J. D. Campos (2005), The influence of the Plata River discharge on the western South Atlantic shelf, *Geophys. Res. Lett.*, *32*, L01603, doi:10.1029/2004GL021638.

1. Introduction

[2] The Plata basin is the fourth largest in the world and covers 20% of the surface of South America (Figure 1). This hydrographic system extends from the subequatorial zone through the tropics, funneling its numerous tributaries into the Plata river (Plata hereafter) whence 22,000 $m^3.s^{-1}$ are discharged into the South Atlantic Ocean and spread along the coasts of Argentina, Uruguay and Brazil (Figure 1). This outflow influences the near-shore ecosystem [*Ciotti et al.*, 1995; *Muelbert and Sinque*, 1996; *Sunyé and Servain*, 1998] and is an important vector for the export of carbon from the continent into the sea [*Degens et al.*, 1991]. In spite of its importance, however, there is only scant information about the fate of the Plata plume after it is entrained into the continental shelf. Historical hydrographic data suggests that in the austral winter (JAS) the Plata plume reaches Cape Santa Marta Grande (~28°S), while in the summer (DJF) it retracts to 32°S [*Piola et al.*, 2000]. There is strong evidence that large precipitation anomalies associated with El Niño (EN) [*Ropelewski and Halpert*, 1987; *Kiladis and Diaz*, 1989] events significantly increase the river discharge [*Depetris et al.*, 1996; *Mechoso and Pérez-Iribarren*, 1992]. The effect of these anomalies on the path of the river plume, however, remains undetermined. We use hydrographic observations, atmospheric reanalysis winds and numerical experiments to discuss the seasonal and interannual variations of the path of the Plata plume over the southwestern Atlantic.

2. Data and Methods

[3] We use historical hydrographic data collected after 1950 and Plata monthly discharge data (Q) for the period 1931–2001 [*Jaime et al.*, 2002]. Wind stress data are from global reanalysis (NCEP [*Kistler et al.*, 2001] and ECMWF [*Trenberth et al.*, 1989]). To validate these global data sets we used wind data from a coastal station at Chui (~33°S). Wind stress was decomposed in cross-shore (τ_x, 125°T) and along-shore (τ_y, 35°T) components. These three wind stress estimates show positive (northeastward) mean values during the austral winter, and negative (southwestward) mean values during the summer.

[4] The numerical experiments were done with the Princeton Ocean Model [*Blumberg and Mellor*, 1987], a 3-D nonlinear primitive equation model with a curvilinear orthogonal coordinate system in the horizontal and a bottom-following (sigma) coordinate in the vertical. The model domain extends from 20 to 55°S and from the coast to 40°W. The model has 25 sigma-levels and a horizontal resolution of ~4 km near the coast. The model included a realistic representation of the bottom topography, was initialized with climatological mean values of temperature and salinity and forced with NCEP winds. The inflows and outflows of the Malvinas (Falkland) and Brazil Currents were obtained from the Parallel Ocean Climate Model (experiment 4C [*Tokmakian and Challenor*, 1999]). The amplitude and phase of the principal tidal constituents are from the Oregon State University TPXO.5 tidal model [*Egbert et al.*, 1994]. The model was spun-up for an initial 3-year period followed by an additional 1-year run for analysis.

3. Analysis

[5] To characterize the seasonal migrations of the Plata over the southwestern Atlantic shelf we compiled sea surface salinity (salinity hereafter) data from a region close to Cape Sta. Marta (Figure 2). Although the seasonal variations of Q are relatively small, the salinity time series shows a distinct seasonal change with a minimum during the winter and a maximum in summer. Since there is no

[1]Departamento Oceanografia, Servicio de Hidrografía Naval, and Departamento Ciencias de la Atmósfera y los Océanos, Universidad de Buenos Aires, Buenos Aires, Argentina.
[2]College of Atmospheric and Oceanic Sciences, Oregon State University, Corvallis, Oregon, USA.
[3]Departamento de Física, Universidad Nacional del Sur and Instituto Argentino de Oceanografía (CONICET), Bahía Blanca, Argentina.
[4]Departamento Física, Fundação Universidade Federal do Rio Grande, Rio Grande, Brazil.
[5]Instituto Ocenaográfico, Universidad de São Paulo, São Paulo, Brazil.

0094-8276/05/2004GL021638$05.00

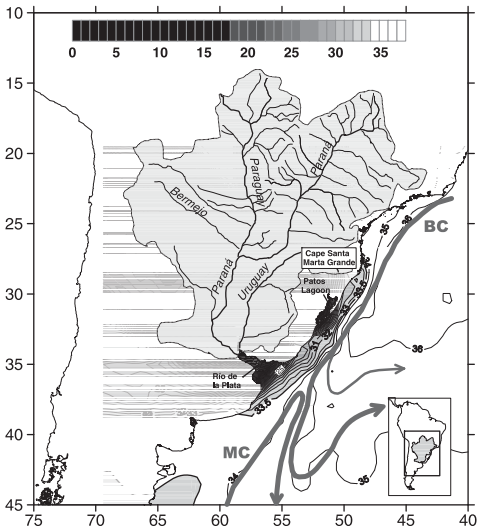

Figure 1. The Plata basin indicating the major tributaries and mean winter surface salinity in the southwest South Atlantic. Contour interval is 1. Salinity <33.5 is shaded in gray. The Brazil Current (BC) and Malvinas Current (MC) are shown schematically.

significant local runoff, and the Patos influence is limited to the region near the mouth [*Zavialov et al.*, 2003], the salinity minimum observed in the bottom panel of Fig. 2 is associated with a northward penetration of the river plume, and the maximum with a retraction. Since the lowest salinities (~30) correspond to periods of southwesterly winds (MJJ), and the highest (~35) to periods of northeasterly winds (DJF), the hydrographic data suggest that the migrations of the Plata plume are highly influenced by the seasonal changes of the wind stress.

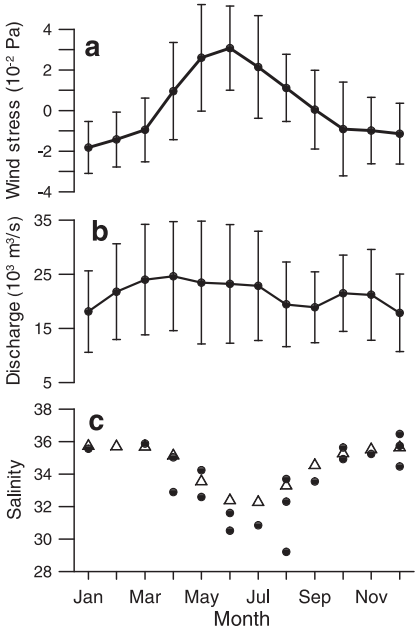

Figure 2. Seasonal variation of (a) alongshore wind stress (Pa), (b) Plata outflow (m^3s^{-1}) and (c) sea surface salinity near Cape Santa Marta Grande from data (●) and model (Δ). The monthly mean values of river outflow and wind stress correspond to the period 1949–2001. The vertical bars indicate standard deviations.

[6] To estimate the influence of the magnitude of the Plata discharge on the meridional penetration of its plume, we computed meridional distributions of nearshore salinity during periods of high and low river discharges (Figure 3). To account for the propagation of the salinity signal associated to outflow variations, based on the results of *Pimenta* [2001], the outflow data was lagged as a function of outflow magnitude and distance to the river mouth. During the periods of high precipitation Q reached 42,000 $m^3.s^{-1}$ (with peaks >60,000 $m^3.s^{-1}$). Conversely, during periods of low precipitation Q decreased to <12,000 $m^3.s^{-1}$. Theoretical arguments indicate that high river discharges should lead to increased plume penetrations [*Garvine*, 1999]. Surprisingly, however, and in spite of the significant discharge variations, the data show similar salinity distributions for the periods of high and low outflow (Figure 3).

[7] The meridional penetration of a river plume is largely controlled by the magnitude of Q and the direction and amplitude of the wind stress forcing [*Kourafalou et al.*, 1996]. To illustrate these relations we computed τ_y and Q for the period 1949–2001 (Figure 4). To eliminate the strong seasonal signal contained in the wind stress, the data was low-passed filtered using a Kaiser filter [*Hamming*, 1977] with a cutoff frequency of 1/14 months. During the period considered there were seven events of high river discharge (Q > 30,000 $m^3.s^{-1}$), five of which were associated with EN events (all but 1959 and 1990). Of these events only one, in 1992, had wind stress conditions favorable for a northward spreading of the river plume. During all the events the wind forcing either opposed the penetration of the plume or was negligible.

4. Numerical Simulations

[8] The above discussion indicates that at interannual time scales the salinity structure in the nearshore region is determined by a balance between the wind stress forcing and the magnitude of the river discharge numerical experiments forced by mean monthly winds show salinity variations in good agreement with the observations. To

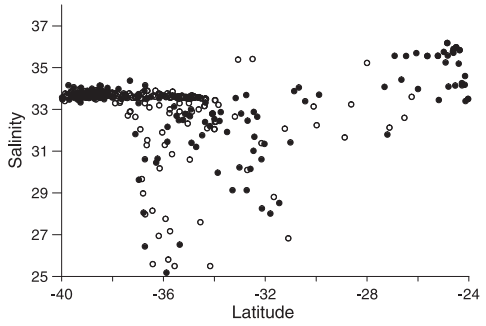

Figure 3. Winter sea surface salinity over the continental shelf as a function of latitude for periods of high river discharge (○, >30000 m^3/s) and low discharge (●, <15000 m^3/s). Outflow data was lagged to account for the delay in propagation of the low salinity signal along the shelf.

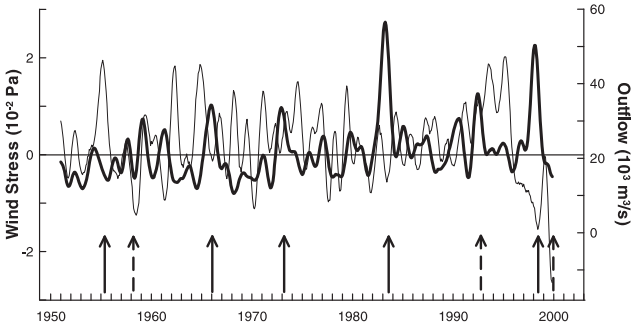

Figure 4. Time series of low frequency river discharge (heavy line, m^3s^{-1}) and along-shore wind stress (thin line, Pa). These data have been low passed filtered to eliminate the strong seasonality in the wind stress. Solid arrows mark periods of large, out of phase fluctuations, and dashed arrows periods of in-phase fluctuations.

investigate the interannual variability we did two numerical experiments. The first experiment emulated the conditions of the 1978 La Niña (LN), during which Q = 12,950 $m^3.s^{-1}$ and τ_y = 0.05 Pa. The second experiment emulated EN conditions from the 1998 event during which Q reached 65,000 $m^3.s^{-1}$ and $\tau_y = -0.025$ Pa. The experiments show the strong control of the wind on the spreading of the river plume (Figure 5). In the LN simulation there is a relatively low salinity coastal strip that extends into the South Brazil Bight (~24°S), about 1400 km from the estuary. In contrast, the simulation replicating EN conditions shows a wider plume that only reaches to 32°S. In this experiment the alongshore spreading of the plume is arrested by the effect of the opposing winds that force the low salinity waters to flow in the offshore direction. In agreement with our data analysis, therefore, the simulations indicate that the meridional spreading of the Plata plume is largely controlled by τ_y.

5. Discussion and Conclusions

[9] The scale of the along-shore plume penetration (L_y) against the opposing summer northeasterly winds can be determined from a simple mass balance between river discharge and the offshore Ekman flow ($Q = \tau_y L_y H_p/D\rho f$). Q = 23,000 $m^3.s^{-1}$, ρ the mean water density (1023 $kg.m^{-3}$), f the Coriolis parameter (7.7 × 10^{-5} s^{-1}), D the Ekman depth (30 m), H_p the plume thickness (10 m) and $\tau_y = -0.02$ Pa. Our balance assumes that the fraction H_p/D of Ekman transport is composed of river water. This simple calculation yields L_y = 270 km, which is a reasonable approximation to the observed extent of the plume. The above results indicate that the meridional migrations of the Plata plume are regulated by the along-shore component of the wind stress forcing. During EN years, Q is significantly augmented by large precipitation anomalies over the river basin. These increases, however, do not lead to a significant northward penetration of the plume due to the arresting effect of τ_y. During these periods, the low salinity waters are displaced offshore. The out-of-phase relation between Q and τ_y anomalies is not fortuitous. The high precipitation anomalies over South America and the northeasterly wind anomalies over the southwestern Atlantic are related to the intensification of the western portion of the South Atlantic high pressure center [*Barros et al.*, 2002; *Silvestri*, 2004]. This intensification leads to low-level, southward advection of warm air along the eastern slope of the Andes, related to the high precipitation anomalies [*Grimm et al.*, 2000] and to the development of southwestward wind anomalies over the southwestern Atlantic shelf (Figure 6).

[10] Although the out-of-phase relation between τ_y and Q is a ubiquitous characteristic of the observations, during a few events they were in phase. During the fall and early winter of 1992, for example, there was a combination of Q = 43,300 $m^3.s^{-1}$ and τ_y = 0.035 Pa. In contrast, in summer of 1999–2000 Q decreased to 12,650 $m^3.s^{-1}$ and $\tau_y = -0.033$ Pa. These events must have lead to exceptionally large fluctuations of the water mass structure. The later is the probable explanation for the anomalous plankton and fish distribution observed in the summer of 2000 [*Mianzan et al.*, 2001]. During the winter of the 1993 EN in-situ observations indicated the existence of a low sea surface temperature (<17°C), salinity (<34), and a persistent northeastward surface drift in the South Brazil Bight [*Campos et al.*, 1996]. The hydrological data indicates that at that time the Plata discharge was only 20,300 $m^3.s^{-1}$. The alongshore

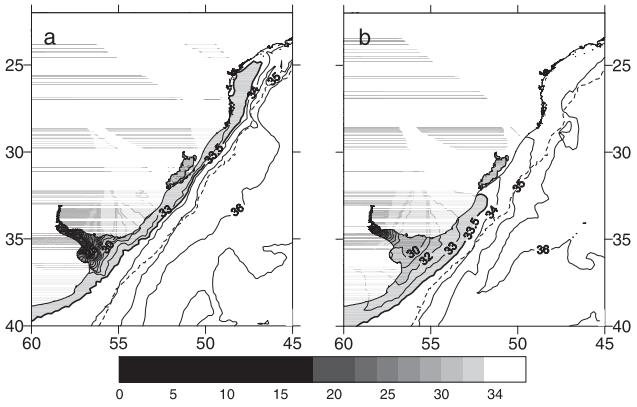

Figure 5. Snapshots of sea surface salinity from the numerical simulations (a) from fall of 1978 and (b) from fall of 1998. Salinity <33.5 is shown in grayscale. The dashed line is the 200 m isobath.

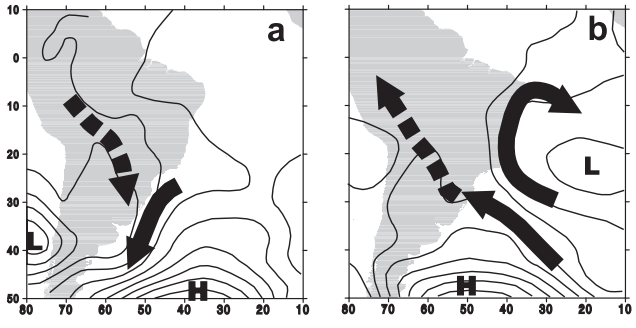

Figure 6. Schematic diagrams of low level atmospheric circulation anomalies relative to neutral periods based on the NCEP reanalysis for the period 1963–1999 associated to (a) EN and (b) LN in AMJ. Arrows indicate wind anomalies and contours geopotential anomalies at 1000 hPa, plotted every 3 gpm.

wind stress anomalies instead were the third largest of the period 1949–2001, only exceeded in the late summer of 1955 and the early fall of 1995, suggesting that the anomalous conditions observed in the South Brazil Bight during the winter of 1993 were associated with southwesterly anomalies in the wind stress forcing.

[11] **Acknowledgments.** This research was funded by the Inter-American Institute for Global Change Research (CRN61), ANPCyT (PICT99 07-06420, Argentina), FAPESP (Brazil), NASA (NAG5 12378 and JPL contract 1206714) and NSF (OCE 0118363). G. Silvestri kindly provided the data to prepare Figure 6.

References

Barros, V. R., A. M. Grimm, and M. E. Doyle (2002), Relationship between temperature and circulation in southeastern South America and its influence from El Niño and La Niña events, *J. Meteorol. Soc. Jpn.*, *80*, 21–32.

Blumberg, A. F., and G. L. Mellor (1987), A description of a three-dimensional coastal ocean circulation model, in *Three-Dimensional Coastal Ocean Models*, *Coastal Estuarine Sci. Ser.*, vol. 2, edited by N. Heaps, pp. 1–16, AGU, Washington D. C.

Campos, E. J. D., J. A. Lorenzzetti, M. R. Stevenson, J. L. Stech, and R. de Souza (1996), Penetration of waters from the Brazil-Malvinas confluence region along the South American continental shelf up to 28°S, *Ann. Acad. Bras. Cienc.*, *68*, 49–58.

Ciotti, A. M., C. Odebrecht, G. Fillmann, and O. O. Möller Jr. (1995), Freshwater outflow and subtropical convergence influence on phytoplankton biomass on the southern Brazilian continental shelf, *Cont. Shelf. Res.*, *15*, 1737–1756.

Degens, E. T., S. Kempe, and J. E. Richey (1991), *Biogeochemistry of Major World Rivers*, John Wiley, Hoboken, N. J.

Depetris, P. J., S. Kempe, M. Latif, and W. G. Mook (1996), ENSO controlled flooding in the Paraná River (1904–1991), *Naturwissenschaften*, *83*, 127–129.

Egbert, G. D., A. F. Bennett, and M. G. G. Foreman (1994), TOPEX/POSEIDON tides estimated using a global inverse model, *J. Geophys. Res.*, *99*, 24,821–24,852.

Garvine, R. W. (1999), Penetration of buoyant coastal discharge onto the continental shelf: A numerical model experiment, *J. Phys. Oceanogr.*, *29*, 1892–1909.

Grimm, A. M., V. R. Barros, and M. E. Doyle (2000), Climate variability in southern South America associated with El Niño and La Niña events, *J. Clim.*, *13*, 35–58.

Hamming, R. W. (1977), *Digital Filters*, Prentice-Hall, Upper Saddle River, N. J.

Jaime, P. R., A. N. Menéndez, M. Uriburu Quirno, and J. A. Torchino (2002), Análisis del régimen hidrológico de los ríos Paraná y Uruguay, *UNDP/GEF, RLA/99/G31*, U. N. Dev. Programme, Ezeiza, Argentina.

Kiladis, G. N., and H. F. Diaz (1989), Global climate anomalies associated with extremes in the Southern Oscillation, *J. Clim.*, *2*, 1069–1090.

Kistler, R., et al. (2001), The NCEP-NCAR 50 year reanalysis: Monthly means CD-ROM and documentation, *Bull. Am. Meteorol. Soc.*, *82*, 247–267.

Kourafalou, V. H., L.-Y. Oey, J. D. Wang, and T. N. Lee (1996), The fate of river discharge on the continental shelf: 1. Modeling the river plume and the inner shelf coastal current, *J. Geophys. Res.*, *101*, 3415–3434.

Mechoso, C. R., and G. Pérez-Iribarren (1992), Streamflow in southeastern South America and the Southern Oscillation, *J. Clim.*, *5*, 1535–1539.

Mianzan, H. W., E. M. Acha, R. A. Guerrero, F. C. Ramírez, D. R. Sorarrain, C. Simionato, and J. Borus (2001), South Brazilian marine fauna in the Río de la Plata estuary, paper presented at IX Congreso Latinoamericano de Ciencias del Mar, Asoc. Latinoam. de Invest. sobre Cienc. del Mar, San Andrés, Colombia.

Muelbert, J. H., and C. Sinque (1996), The distribution of bluefish larvae (*Pomatomus saltatrix*) in the continental shelf of southern Brazil, *Mar. Freshwater Res.*, *47*, 311–314.

Pimenta, F. M. (2001), Estudo numerico da influencia da descarga fluvial e dos ventos sobre dinamica da pluma do Rio da Prata, M.S. thesis, Univ. de São Paulo, São Paulo, Brazil.

Piola, A. R., E. J. D. Campos, O. O. Möller Jr., M. Charo, and C. M. Martinez (2000), Subtropical shelf front off eastern South America, *J. Geophys. Res.*, *105*, 6566–6578.

Ropelewski, C. H., and S. Halpert (1987), Global and regional scale precipitation patterns associated with El Niño/Southern Oscillation, *Mon. Weather Rev.*, *115*, 1606–1626.

Silvestri, G. E. (2004), El Niño signal variability in the precipitation over southeastern South America during austral summer, *Geophys. Res. Lett.*, *31*, L18206, doi:10.1029/2004GL020590.

Sunyé, P. S., and J. Servain (1998), Effects of seasonal variations in meteorology and oceanography on the Brazilian sardine fishery, *Fish. Oceanogr.*, *7*, 89–100.

Tokmakian, R., and P. G. Challenor (1999), On the joint estimation of model and satellite sea surface height anomaly errors, in *Ocean Modell.*, *1,* pp. 39–52, Hooke Inst. Oxford Univ., Oxford, U. K.

Trenberth, K., J. Olson, and W. Large (1989), *A Global Ocean Wind Stress Climatology Based on ECMWF Analyses*, *Tech. Rep. NCAR/TN-338+STR*, Natl. Cent. for Atmos. Res., Boulder, Colo.

Zavialov, P. O., A. G. Kostianoy, and O. O. Moller Jr. (2003), SAFARI cruise: Mapping river discharge effects on southern Brazilian shelf, *Geophys. Res. Lett.*, *30*(21), 2126, doi:10.1029/2003GL018265.

E. J. D. Campos, Instituto Ocenaográfico, Universidad de São Paulo, Cidade Universitaria, 05508-900 São Paulo, Brazil.

R. P. Matano, College of Atmospheric and Oceanic Sciences, Oregon State University, Corvallis, OR 97331-5503, USA.

O. O. Möller Jr., Departamento Física, Fundação Universidade Federal do Rio Grande, 96201-900 Rio Grande, Brazil.

E. D. Palma, Departamento de Física, Universidad Nacional del Sur and Instituto Argentino de Oceanografía (CONICET), Av. Alem 1253, 8000 Bahía Blanca, Argentina.

A. R. Piola, Departamento Oceanografia, Servicio de Hidrografía Naval and Dept. Ciencias de la Atmósfera y los Océanos, Universidad de Buenos Aires, Av. Montes de Oca 2124, 1271 Buenos Aires, Argentina. (apiola@hidro.gov.ar)